

# Mechanism of destruction of benzoyl peroxide on surface of $sp^2$ -type carbon nanomaterials

Mykola Kartel<sup>1,2</sup>, Liudmyla Karachevtseva<sup>2,3</sup>, Wang Bo<sup>2</sup>, Daryna Haliarnyk<sup>1</sup>, Olga Bakalinska<sup>1</sup>, Tetyana Kulyk<sup>1</sup>, Borys Palyanytsya<sup>1</sup>, Yevgen Demianenko<sup>1</sup>, Anatoliy Grebenyuk<sup>1</sup>, Volodymyr Kuts<sup>1</sup>

<sup>1</sup>Department of Nanoporous and Nanosized Carbon Materials, O. Chuiko Institute of Surface Chemistry, NAS of Ukraine, 17 General Naumov Street, Kyiv 03164 Ukraine;

<sup>2</sup>China-Central and Eastern Europe International Science and Technology Achievement Transfer Center, Ningbo University of Technology, 201 Fenghua Road, Ningbo 315211, China;

<sup>3</sup>Department of Photonic Crystals, V. Lashkaryov Institute of Semiconductor Physics, NAS of Ukraine, 41 Prospect Nauki, Kyiv 03028, Ukraine.

DOI: 10.5185/amlett.2018.1965

www.vbripress.com/aml

## Abstract

The possible mechanisms of decomposition of benzoyl peroxide were investigated by the method of density functional theory with the exchange-correlation functionality of B3LYP, a basis set of 6-31G (d, p). It was carried out a comparative analysis of the quantum chemical calculations of the electronic structure of carbon nanoclusters simulating the active surface of  $sp^2$  carbon materials, including their modifications by the heteroatoms N and O. The energy parameters of the benzoyl peroxide molecule and all possible products of its decomposition, as well as the interaction of the free radical Ph-COO• with model graphite-like nanoclusters were considered. The calculations are compared with the experimental results of the catalytic activity of the varieties of activated charcoal and the catalase enzyme in the reaction of the benzoyl peroxide decomposition in a non-aqueous medium. It has been established that in the benzoyl peroxide molecule, regardless of the polarity of the medium, the weakest is the bond (O-O). The greatest ability to decompose benzoyl peroxide, which is much larger than that of catalase, was detected on the N-containing carbonaceous materials. It is shown that the free radical Ph-COO• is lighter and kinetically, and thermodynamically interacted with the graphite-like plane of the model N-containing carbon nanoclusters. Copyright © 2018 VBRI Press.

**Keywords:** Carbon materials, benzoyl peroxide, catalytic activity, reaction mechanism, quantum chemistry, density function theory method, cluster approximation.

## Introduction

It is known that nanoporous and nanodispersed carbon materials (CM) have the properties of catalysts in many chemical processes of red-ox and acid-base types (halogenation, dehydrogenation, decomposition, oxidation-reduction, etc.) [1]. Catalytic activity of the CM is depended on both the structural and sorption characteristics (specific surface area, nature of porosity), and surface chemistry (the presence of heteroatoms in the structure of the carbonaceous matrix, surface functional groups of acid or basic nature) [2]. CM are able to influence on the variety of biologically important processes that make up the metabolic pathways of living organisms. The researches have established that the therapeutic action of the CM is related not only to its absorption properties, but also to the effect on the enzymatic processes (hydrolysis of proteins, fats and esters, sucrose inversions, decomposition of hydrogen peroxide, urea, etc.), that is, carbonaceous materials exhibit enzyme-like properties [3]. Several papers [4-7]

showed that the decomposition of hydrogen peroxide on the surface of a  $sp^2$ -type carbon cluster (activated carbon surface, exfoliated graphite, fullerenes, nanotubes, nanohorns, graphene, etc.) is carried out by transferring the electronic density from the cluster to peroxide molecule in the formed complexes "carbon cluster- $H_2O_2$ ". Such a transfer leads to the collapse of the peroxide molecule, since the formation of anions  $OH^-$  is more energetically efficient. The mechanism of the process is represented as the homolytic decay of the  $H_2O_2$  molecule by the O-O bond onto two free radicals  $\cdot OH$ , which are sufficiently strong electron acceptors (affinity energy 1.825 eV). Additional possibility for radicals  $\cdot OH$  is an interaction with a free radical fragment of a carbon cluster with the formation of a chemical bond (the formation of phenolic groups on the surface of the CM). In such systems, the rate of decomposition reaction is determined by the ionization potential (or work of the electron output, or magnitude of the energy of the upper occupied molecular orbital) of the carbon cluster.

Recently, the attention of researchers attracts the use of enzymes in non-aqueous media, since a number of practically important organic peroxides and hydroperoxides are not water soluble [8-10]. Therefore, we consider interesting and relevant studies of the enzyme-like activity of CM in non-aqueous solutions.

The purpose of this work is to study the mechanism of decomposition of organic peroxide on the example of benzoyl peroxide (BP) on the basis of quantum chemical calculations of the molecular structure in different media, as well as to simulate the interaction of the benzoate-radical PhCOO• (product of BP decay) with model sp<sup>2</sup> carbon nanoclusters, which include N- and O-heteroatoms. Results of calculations are compared with experimental data of the BP decomposition in the presence of the samples of activated carbon KAU and its N- and O-modified forms [11].

## Experimental

To establish the mechanism of the influence of the electronic structure of the CM on the BP decomposition, it is carried out the quantum-chemical calculations of the energy of the bonds in the molecule of the peroxide itself Ph-(CO)-O-O-(OC)-Ph, located in different media, and the interaction of the free radical PhCOO• formed during the homolytic breakdown of the BP peroxide group with graphite-like planes of model carbon nanoclusters, including ones with inclusion in the structure of a certain number of N- and O-heteroatoms. Calculations were made using the US GAMESS program [12] by the theory of function density with the exchange-correlation functional B3LYP [13, 14] with the use of the dispersion correction [15] and the base set 6-31G (d, p). The solvent medium was modeled in the approximation of the continuum solvent model (polarization continuum model, PCM) [16]. The free energy of physical adsorption ( $\Delta G_{phs}$ ) was calculated as the difference between the total energy of the physically adsorbed complexes [PhCOO•...CM] and the sum of the total energies of the individual radicals [PhCOO•] and graphite-like clusters [CM], taking into account the corresponding thermodynamic corrections:

$$\Delta G_{phs} = G_{298}^0[\text{PhCOO}\cdot\text{...CM}] - G_{298}^0[\text{PhCOO}\cdot] - G_{298}^0[\text{CM}].$$

The activation energy was defined by the formula:  $\Delta G_{act} = G_{298}^0$  (transition state) -  $G_{298}^0$  (reactants), and the energetic effect of the reaction ( $\Delta G_{re}$ ), respectively:

$$\Delta G_{re} = G_{298}^0$$
 (reaction products) -  $G_{298}^0$  (reactants),

where  $G_{298}^0 = E_t + ZPE + G_{0 \rightarrow 298K}$ , in which  $E_t$  is the total energy of the corresponding optimized structure, and the energy of zero oscillations (ZPE) and the correction value  $G_{0 \rightarrow 298K}$  were found by calculating the Hessian matrix of each of these states. For the reliability of the found energy minima and transition states on hypersurface of potential energy, a verification was carried out in accordance with the Merrell-Leydler theory with the additional calculation of the Hesse matrix [17], which allows to determine

thermodynamic and kinetic characteristics (free energy of physical sorption  $\Delta G_{phs}$ , chemisorption  $\Delta G_{chs}$  and Gibbs' activation  $\Delta G_{act}$ ) for reaction of the interaction of the radical PhCOO• with graphite-like planes of model nanoclusters at 298 K.

For objective interpretation of the results of quantum-chemical calculations, they were compared with the data of experimental studies of BP decomposition on samples of activated carbon KAU and its two modifications - oxidized (O-KAU) and nitrogen-containing (N-KAU) ones obtained by treatment of 30% solution of nitric acid and by calcination of urea soaked oxidized carbon [11]. Characteristics of samples are presented in Table 1 [11, 18].

**Table 1.** Elemental composition, surface chemistry, structural-sorption and catalytic properties of carbon materials on the basis of activated carbon KAU.

Parameters	Samples of CM		
	KAU	O-KAU	N-KAU
Elemental composition, wt.% (at.%):			
Carbon	<b>99.4 (97.3)</b>	96.2 (86.4)	89.2 (72.3)
Hydrogen	0.2 (2.4)	1.1 (11.8)	<b>2.3 (22.3)</b>
Oxygen	0.1 (0.1)	2.1 (1.4)	<b>6.2 (3.8)</b>
Nitrogen	0.3 (0.2)	0.6 (0.4)	<b>2.3 (1.6)</b>
Functional surface groups, meq/g:			
Carboxylic	0.04	<b>0.84</b>	0
Lactonic	0.06	0.20	<b>0.45</b>
Phenolic	0.02	<b>1.39</b>	0.05
Total acidic	0.12	<b>2.43</b>	0.50
Total basic	0	0	<b>1.90</b>
Structural sorption characteristics:			
Pore volume ( $V_s$ ), cm <sup>3</sup> /g	0.50	0.85	<b>0.90</b>
BET surface area ( $S_{sp}$ ), m <sup>2</sup> /g	920	790	<b>940</b>
Average pore radius ( $\bar{r}$ ), nm	2.1	2.2	<b>2.0</b>
Catalytic activity on BP decomposition*:			
Michaelis' constant, mM/L	480	1120	<b>30</b>
Coefficient of affinity	2.1·10 <sup>-3</sup>	8.9·10 <sup>-4</sup>	<b>3.3·10<sup>-2</sup></b>

\*The catalytic ability of CM in relation to the decomposition of BP were determined and compared with the activity of catalase by the method of studying the kinetic regularities of the course of enzymatic reactions over the Michaelis' constants ( $K_M$ ) [18]. These constants were determined from the dependences of Laynuiver - Burk in the double inverse coordinates of the initial reaction rate and the concentration of the substrate (BP solutions in ethyl acetate) [19]. For catalase  $K_M$  in this reaction was 340 mmol/L (coefficient of affinity 2.9·10<sup>-3</sup>).

The analysis of the reaction products of the BP decomposition was carried out by the method of TPD mass-spectrometry [20] in the range 1-210 a.m.u. The most probable products corresponding to certain masses are given in Table 2.

**Table 2.** Probable products of the catalytic benzoyl peroxide decomposition on the carbon materials (samples of activated carbons KAU) according to the temperature-programmable mass-spectrometry.

m/z	Products
17, 18	·OH, H <sub>2</sub> O
28	CO
44	CO <sub>2</sub>
77	Ph·
105	PhCO·
121, 122	PhCOO·, PhCOOH

## Results and discussion

The experimental data presented in the methodical part show that the catalytic activity of CM (activated carbon of KAU and its modifications) in the BP decomposition is significantly increased ( $K_M$  decreases) with increasing volume of sorption pores ( $V_S$ ) and specific surface area of ( $S_{sp}$ ), and, vice versa, with a decrease in the average pore radius ( $\bar{r}$ ). But the greatest influence on catalytic activity is observed from the presence of N- and O-heteroatoms. Thus, the introduction of N-atoms into the carbon matrix increases, and O-atoms (in the form of surface groups of acidic nature) decreases the catalytic activity of CM in the BP decomposition. Similar patterns were observed in works [6, 7, 21] at study of  $H_2O_2$  decomposition by different nitrogen and oxygen-containing CM. It should also be noted that the enzyme-like ability of N-containing carbon in a non-aqueous medium was on the order higher than activity of native catalase. This gives us reason to suppose that the activity of CM in the reactions of the BP decomposition in non-aqueous media will be equally determined by the electron-donor ability of a carbon catalyst, namely, its ionization potential  $I_p$  (or the work of electron output  $A_e$ , or the energy level of upper occupied molecular orbital of the  $E_{HOMO}$ , etc.).

### Quantum-chemical study of homolytic degradation of benzoyl peroxide

The calculations for optimization of the structure and energy parameters of the BP molecule and all possible products obtained at breakage of bonds are made. In particular, it is considered the homolytic coupling of O–O (1) (Fig. 1a) with the formation of two free radicals  $PhCOO\cdot$ , the relative molecular weight of which is 121 a.m.u. In turn (Fig. 1b), radical  $PhCOO\cdot$  can homolytically decompose onto phenyl-radical  $Ph\cdot$  (77 a.m.u.) with the release of  $CO_2$  molecule (44 a.m.u.).

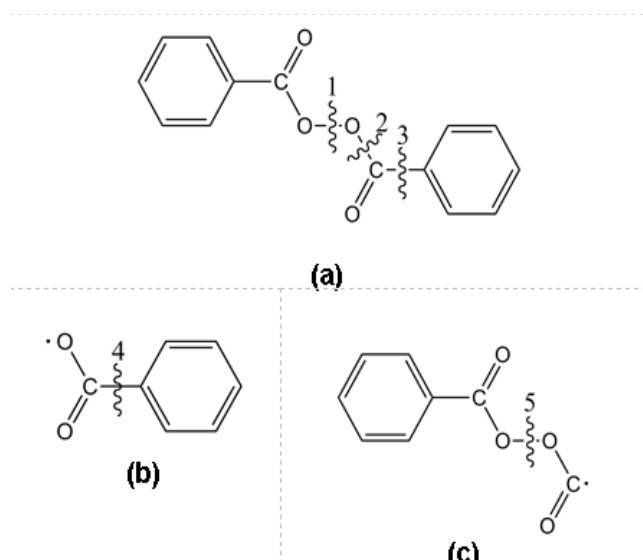


Fig. 1. Possible ruptures of covalent bonds in the molecule BP (a) and products of its decomposing (b, c) by the homolytic mechanism.

The BP molecule can also decompose with coupling O–C (2) (Fig. 1a) onto two free radicals  $PhCOOO\cdot$  and  $PhCO\cdot$  with respective molecular weight of 137 and 105 a.m.u. The first of these can be disintegrated with the formation of molecule  $O_2$  and a free radical  $PhCO\cdot$ , which, in turn, can decompose with the breakdown of the C–C bond to the molecule CO (28 a.m.u.) and phenyl radical  $Ph\cdot$ . It is also possible a breakage of the C–C bond (3) (Fig. 1a). In this case, the phenyl radical  $Ph\cdot$  and the radical  $PhCOOOCO\cdot$  with a weight of 165 a.m.u. can be formed. The last, like the preceding one, can decay with the break-up of the O–O bond (5) (Fig. 1c) and the formation of the  $PhCOO\cdot$  radical and molecule  $CO_2$ . It should be noted that the radical  $PhCOOOCO\cdot$  (Fig. 1c) did not succeed in locating in general, since optimizing the structure of it lead to increase of the interatomic distance of the O–O linkage (5) to 2.5 Å and more, which in effect means its breaking and formation of radical  $PhCOO\cdot$  and molecule  $CO_2$ . Consequently, the absence in the experimental TPD of mass spectra of a fragment with a mass number of 165 a.m.u. is explained by the theoretically predicted thermodynamic instability of the mentioned radical (Fig. 1c).

The results of calculations on the values of the energy of bond breaks in the BP molecule are summarized in Table 3. As can be seen, regardless of the medium chosen for calculating, in the BP molecule the bond O–O is weakest (Fig. 1a), and this results to the formation of two radicals  $PhCOO\cdot$ . Significantly stronger bond is between the carboxyl group and benzene ring C–C (3) (Fig. 1a). The strongest link is O–C (2) between the peroxide oxygen and carbon of the carboxyl group (Fig. 1a). The thermodynamic probability of its rupture is the lowest, which is confirmed by the absence in the experimental TPD of the mass spectrum of a fragment with a mass number of 137.

Table 3. The values of the energy of breaking of bonds in the molecule of benzoyl peroxide in different media (kJ/mol).

Media ( $\mu$ ; $\epsilon$ )	Energy of breakage, kJ/mol			
	O-O (1)	O-C (2)	C-C (3)	C-C (4)
Ethyl acetate (6.1; 1.81)	92.55	319.5	120.6	22.4
Acetone (20.9; 2.84)	96.71	326.2	123.1	25.7
Carbon tetrachloride (2.2; 0)	101.3	329.7	123.7	25.9
Butanol (17.1; 1.66)	104.5	327.9	136.8	22.6
Acetic acid (6.19; 1.74)	114.9	335.6	147.2	20.5
Vacuum (1; 0)	105.5	392.2	123.5	18.2

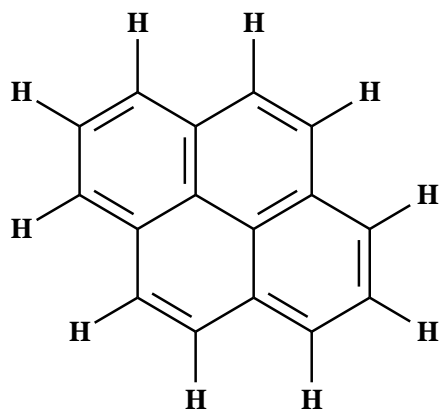
Thus, with the breakdown of the bond C–C (3), four products of BP decomposition can be formed - stable molecules CO and  $CO_2$  (28 and 44 a.m.u.) and two free radicals  $PhCOO\cdot$  and  $Ph\cdot$  (105 and 77 a.m.u.), which can take part in interaction with CM.

The obtained results suggest that homolytic degradation of the BP molecule, irrespective of the medium, is most likely to be decomposed into two  $PhCOO\cdot$  radicals, which subsequently interact with nanoclusters of CM surface or decompose on the phenyl radical  $Ph\cdot$  and the molecule  $CO_2$ .

**Quantum-chemical study of the interaction of free radical  $\text{PhCOO}\cdot$  with graphite-like nanocluster of CM**

Coming from the elemental composition, structural-sorption characteristics and the nature of the surface functional groups of the studied CM (Table 1), it is practically impossible to uniquely propose universal structures that would simulate the reagent plots of the carbonaceous catalyst surface. The chemical composition of real catalysts involves the presence of four basic elements: C, H, O and N. Their ratio can vary widely, and this affects the identity and properties of the CM. Thus, a small percentage of H, O, and N in the material make it possible to consider as pure carbon. A significant percentage of H converge material to organic compounds of polyaromatic type. A high content of O in the material causes the presence of an independent class of substances called oxidized CM (oxidized carbon, oxidized graphite, oxidized graphene, oxidized nanotubes, etc.), and they are often considered as carbonaceous cation exchangers. Finally, CM with a high content of N (nitrogen-containing materials) are known as having an increased basicity and appear anion exchange and electron-donating properties.

It is known from experiment [11] that oxidation of CM leads to decrease, while nitrogenation of carbon matrix to increase of their catalytic activity in the reactions of decomposition of hydrogen peroxide, benzoyl and lauryl peroxides, etc. Typically, the value of the catalytic activity of the studied CM correlates with their electron donor capacity, which is quantified by physical parameters: ionization potential ( $I_p$ ), work of electron output ( $A_e$ ), energy level of upper occupied molecular orbitals ( $E_{HOMO}$ ) for the corresponding model nanoclusters. It should be emphasized that the results of the calculation of  $I_p$  for model of carbon nanoclusters, which simultaneously contain N- and O-atoms, strongly depends on their number and location. The value of  $I_p$  can be either smaller or greater than the ionization potential of pure carbon nanoclusters [21]. For the pure carbon structure of planar ( $sp^2$ ) carbon nanoclusters the polyaromatic structure  $\text{C}_{16}\text{H}_{10}$  (calculated  $I_p = 5.246$  eV) was used:



Since oxidation and nitrogenation of the CM leads to the formation of O-, N-, and mixed O, N-containing products, their surface was modeled by appropriate O-, N-, and mixed N, O-containing nanoclusters. Selective structures are presented in Fig. 2. They are grouped so that the first group of them (1) - (6) has calculated values of  $I_p$  less, and the second group (7) - (12) more than for pure carbon nanoclusters  $\text{C}_{16}\text{H}_{10}$ . The results of calculations are presented in Table. 4

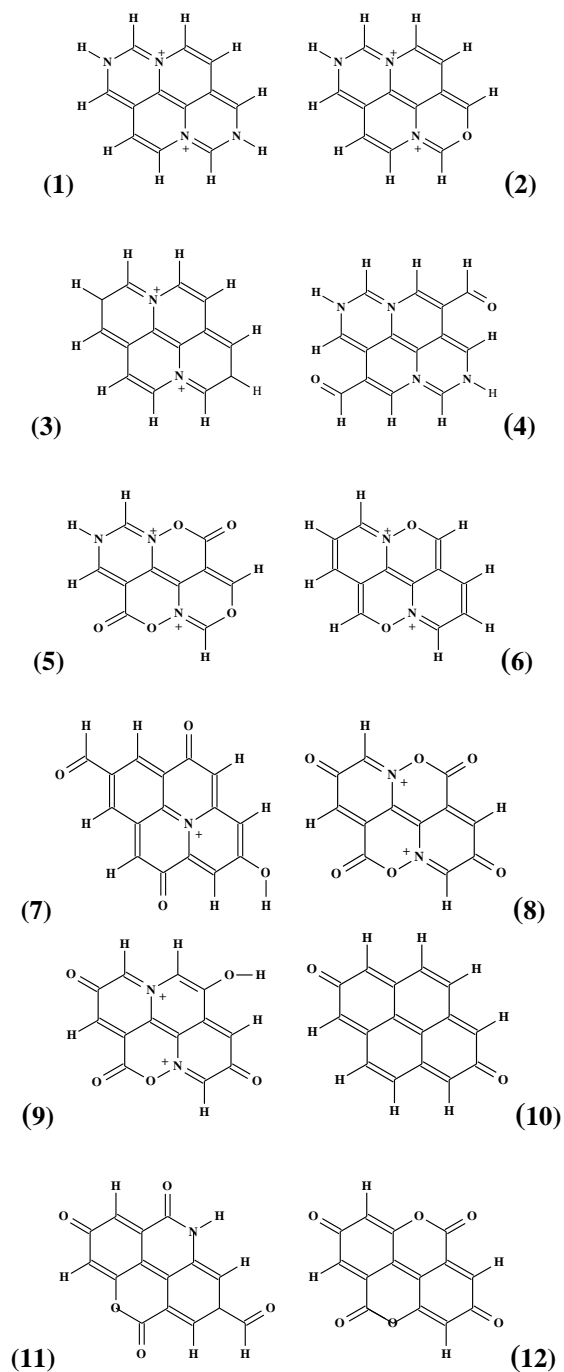


**Fig. 2.** Structures of carbon nanoclusters that simulate possible active plots of the carbon materials surface.

**Table 4.** Calculated data for model nanoclusters (1) - (12).

N	Formula	Elemental content, at. %				$I_p$ , eV
		C	H	O	N	
1	C <sub>12</sub> N <sub>4</sub> H <sub>10</sub>	46.2	38.5	-	15.3	2.425
2	C <sub>12</sub> N <sub>3</sub> O <sub>1</sub> H <sub>9</sub>	48	36	4	12	2.748
3	C <sub>14</sub> N <sub>2</sub> H <sub>10</sub>	53.8	38.5	-	7.7	3.108
4	C <sub>14</sub> N <sub>4</sub> O <sub>2</sub> H <sub>10</sub>	46.7	33.3	6.7	13.3	3.241
5	C <sub>10</sub> N <sub>3</sub> O <sub>5</sub> H <sub>5</sub>	43.5	21.7	21.7	13.1	3.344
6	C <sub>12</sub> N <sub>2</sub> O <sub>2</sub> H <sub>8</sub>	50	33.3	8.3	8.3	3.589
	C <sub>16</sub> H <sub>10</sub>	61.5	38.5	-	-	5.246
7	C <sub>16</sub> N <sub>1</sub> O <sub>4</sub> H <sub>8</sub>	55.2	27.6	13.8	3.4	5.791
8	C <sub>12</sub> N <sub>2</sub> O <sub>6</sub> H <sub>4</sub>	50	16.7	25	8.3	5.932
9	C <sub>13</sub> N <sub>2</sub> O <sub>5</sub> H <sub>6</sub>	52	20	20	8	6.057
10	C <sub>16</sub> O <sub>2</sub> H <sub>8</sub>	61.5	30.8	7.7	-	6.370
11	C <sub>15</sub> N <sub>1</sub> O <sub>5</sub> H <sub>6</sub>	55.6	22.2	18.5	3.7	7.037
12	C <sub>14</sub> O <sub>6</sub> H <sub>4</sub>	58.3	16.7	25	-	7.334

On the Fig. 3 a diagram clearly demonstrates the dependence of the ionization potential of the calculated nanoclusters on the content of N- and O-atoms in them.

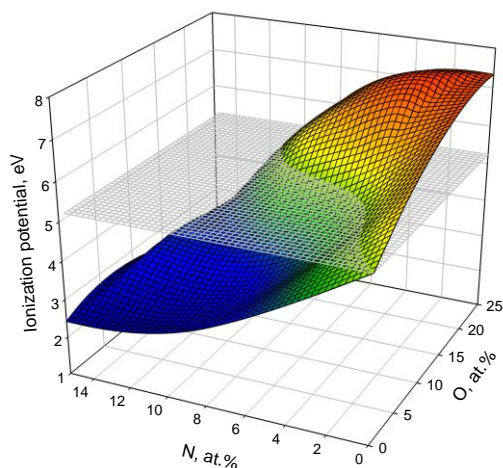


**Fig. 3.** The dependence of the ionization potential (in eV) of nanoclusters from the content (in at. %) in them of N- and O-heteroatoms. The plane shows the potential value of polyaromatic structure C<sub>16</sub>H<sub>10</sub> that used as a model of pure carbon nanocluster ( $I_p = 5.246$  eV).

From Table 4 and Fig. 2 it can be seen that the structure (1) - (6) are N- and N, O-containing nanoclusters, which have higher electron-donor ability than pure carbon nanoclusters C<sub>16</sub>H<sub>10</sub>. Average value  $I_p$  for these structures is  $3,08 \pm 0,33$  eV, which is very close to the magnitude of ionization potential of nanocluster (3) - C<sub>14</sub>N<sub>2</sub>H<sub>10</sub> (3,108 eV). Structures (7) - (12) represent O- and O, N-containing nanoclusters that have lower electron-donor ability than pure carbon. The average value  $I_p$  for them is  $6.42 \pm 0.51$  eV, which is close to the magnitude of the potential of the nanocluster (10) - C<sub>16</sub>O<sub>2</sub>H<sub>8</sub> (6.370 eV). Therefore, for a detailed definition of the thermodynamic and kinetic characteristics of the interaction of free radicals PhCOO• with graphite-like

planes of pure carbon, nitrogen- and oxygen-containing materials we selected nanoclusters, accordingly, C<sub>16</sub>H<sub>10</sub>, C<sub>16</sub>O<sub>2</sub>H<sub>8</sub> and C<sub>14</sub>N<sub>2</sub>H<sub>10</sub>.

On the basis of quantum-chemical calculations it was established that the interaction of the graphite-like plane of the CM with the radical PhCOO• takes place in two stages:

- (1) Formation of a physically adsorbed complex [PhCOO•...CM]<sub>phys</sub>;
- (2) Formation (after overcoming the energy barrier of the transition state [PhCOO•...CM]<sub>act</sub>) chemical bond between the reactants [PhCOO•-CM]<sub>chs</sub>.

The structure of corresponding nanocomplex (on example of O-containing carbon nanocluster C<sub>16</sub>O<sub>2</sub>H<sub>8</sub> and radical PhCOO•) is shown in Fig. 4. For N-containing and pure carbon nanoclusters the structures of the complexes are similar. The resulting thermodynamic ( $\Delta G_{phys}$ ,  $\Delta G_{chs}$ ) and kinetic ( $\Delta G_{act}$ ) characteristics of the interaction radical PhCOO• and nanoclusters C<sub>16</sub>H<sub>10</sub>, C<sub>16</sub>O<sub>2</sub>H<sub>8</sub> and C<sub>14</sub>N<sub>2</sub>H<sub>10</sub> are presented in Table 5.

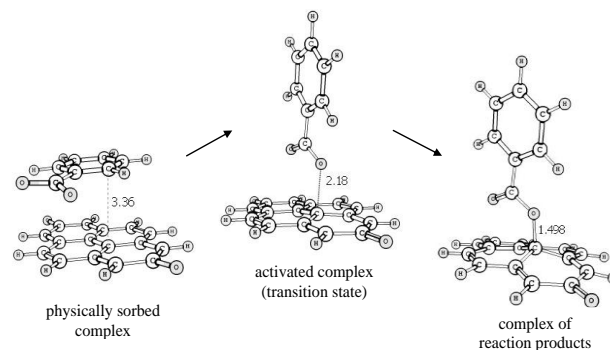


**Fig. 4.** Scheme of interaction of the radical PhCOO• with the nanocluster C<sub>16</sub>O<sub>2</sub>H<sub>8</sub>.

**Table 5.** Thermodynamic ( $\Delta G_{phys}$ ,  $\Delta G_{chs}$ ) and kinetic ( $\Delta G_{act}$ ) characteristics of the interaction of the PhCOO• radical with carbon nanoclusters.

Nanocluster	Ionization potential, eV	$\Delta G_{phys}$ , kJ/mol	$\Delta G_{act}$ , kJ/mol	$\Delta G_{chs}$ , kJ/mol
C <sub>14</sub> N <sub>2</sub> H <sub>10</sub>	3,108	-18,7	4,8	-5,30
C <sub>16</sub> H <sub>10</sub>	5,246	-13,5	37,6	-6,60
C <sub>16</sub> O <sub>2</sub> H <sub>8</sub>	6,370	-12,0	35,9	-6,67
	X	Y <sub>1</sub>	Y <sub>2</sub>	Y <sub>3</sub>
	R <sup>2</sup> (Y <sub>i</sub> = a <sub>i</sub> + b <sub>i</sub> X)	0,990	0,876	0,930

As it can be seen from Table 5, the strongest physically adsorbed complex is [PhCOO•...C<sub>14</sub>N<sub>2</sub>H<sub>10</sub>]<sub>phys</sub>, since such system has most negative value of the energy of physical adsorption  $\Delta G_{phys}$ . In such complexes the surface of radical PhCOO• is almost parallel to the graphite-like plane of the nanocluster (Fig. 4). The formation of the chemisorption complex [PhCOO•-C<sub>14</sub>N<sub>2</sub>H<sub>10</sub>]<sub>chs</sub> occurs through the formation of a transition state [PhCOO•...C<sub>14</sub>N<sub>2</sub>H<sub>10</sub>]<sub>act</sub>, in which the radical is coordinated with the plane of the nanocluster by

one of the oxygen atoms of the group  $\text{-COO}\cdot$ . The reliability of the existence of transition states is confirmed by the presence of one imaginary vibration mode ( $\text{iv}_v$ ) that corresponds to the transition vector, which characterizes the direction of the coordinate shifts of atomic nuclei at the transition from the starting materials to the reaction products.

According to the results of quantum chemical calculations, the chemisorption of radical  $\text{PhCOO}\cdot$  is most easily carried out on the N-containing  $\text{C}_{14}\text{N}_2\text{H}_{10}$  nanoclusters, since it requires the lowest activation energy  $\Delta G_{act}$  (4.8 kJ/mol), while for nanoclusters  $\text{C}_{16}\text{H}_{10}$  and  $\text{C}_{16}\text{O}_2\text{H}_8$  the activation energy  $\Delta G_{act}$  is much higher (37.6 and 35.9 kJ/mol, respectively). It is also clear from **Table 5** that the highest value of the thermodynamic effect of  $\text{PhCOO}\cdot$  chemisorption is observed on nanocluster  $\text{C}_{14}\text{N}_2\text{H}_{10}$  with  $\Delta G_{chs} = -5.3$  kJ/mol, in comparison with similar values for  $\text{C}_{16}\text{H}_{10}$  and  $\text{C}_{16}\text{O}_2\text{H}_8$ . This means that the surface of the N-containing carbon catalysts will be the easiest to regenerate for the next chemisorption acts of benzoyl decomposition products, first of all with  $\text{PhCOO}\cdot$  radical.

## Conclusion

In the benzoyl peroxide molecule, the weakest bond is (O–O), due to the rupture of which the formation of two radicals  $\text{C}_6\text{H}_5\text{-COO}\cdot$  is most likely to be. Radicals, in turn, are able to decompose with the formation of a phenyl radicals ( $\cdot\text{C}_6\text{H}_5$ ) and  $\text{CO}_2$  molecules.

Thermodynamic ( $\Delta G_{phs}$ ,  $\Delta G_{chs}$ ) and kinetic ( $\Delta G_{act}$ ) characteristics of the interaction of  $\text{PhCOO}\cdot$  radical with carbon nanoclusters are determined by their electron-donor ability (ionization potential). In non-aqueous media (solutions) nitrogen-containing carbon materials have significantly higher catalytic activity compared to the enzyme catalase.

## Acknowledgements

This work was supported by the Project of the Swedish Research Council (VR) under contract #348-2014-4250, Contract of Employment/Letter of Intent of 2014.12.01 of the Ningbo University of Technology (China) and Project of the National Academy of Sciences of Ukraine Program of Fundamental Research “New Functional Substances and Materials for Chemical Engineering”.

## Author's contributions

*Conceived the plan:* M. Kartel, D. Haliarnyk, V. Kuts; *Performed the experiments:* D. Haliarnyk, O. Bakalinska, Wang Bo, T. Kulyk, B. Palyanytsya; *Data analysis:* L. Karachevtseva, Ye. Demianenko, A. Grebenyuk, V. Kuts; *Wrote the paper:* M. Kartel, D. Haliarnyk, V. Kuts. Authors have no competing financial interests.

## References

1. Fidalgo, B.; Menendez, J. A.; *Chinese J. Catal.*, **2011**, 32, 207.  
DOI: [https://doi.org/10.1016/S1872-2067\(10\)60166-0](https://doi.org/10.1016/S1872-2067(10)60166-0)
2. Trogadas, P.; Fuller, T. F.; Strasser, P.; *Carbon*, **2014**, 75, 5.  
DOI: [10.1016/j.carbon.2014.04.005](https://doi.org/10.1016/j.carbon.2014.04.005)
3. Stavitskaya S. S.; Strelko V. V.; *Theoret. Experim. Chem.*, **1995**, 31, 65.
4. Lapko, V. F.; Gerasimyuk, I. P.; Kuts, V. S.; Tarasenko, Yu. A.; *Russ. J. Phys. Chem. A*, **2010**, 84, 934.
5. Voitko, K.; Tóth, A.; Demianenko, E.; Dobos, G.; Berke, B.; Bakalinska, O.; Grebenyuk, A.; Tombácz, E.; Kuts, V.; Tarasenko, Yu.; Kartel, M.; László, K.; *J. Coll. Inter. Sci.*, **2015**, 437, 283.
6. Kuts, V. S.; Gerasimyuk, I. P.; Tarasenko, Yu. A.; *Chemistry, Physics and Technology of Surface*, Kiev: Naukova dumka, **2009**, 15, 25. [in Russian].
7. Voitko, K. V.; Demianenko, E. N.; Bakalinska, O. N.; Tarasenko, Yu. A.; Kuts, V. S.; Kartel, N. T.; *Chem. Phys. Technol. Surf.*, **2013**, 4, 3. [in Ukrainian].  
DOI: <https://doi.org/10.15407/hftp04.01>
8. Lee, M.-Y.; Dordick, J. S.; *Current Opinion in Biotechnology*, Elsevier Current Trends, **2002**, 13, 376.
9. Krieger, N.; Bhatnagar, T.; Baratt, J. C.; Baron A. M.; de Lima, V. M.; Mitchell, D.; *Food Technol. Biotechnol.*, **2004**, 42, 279.
10. Dimcheva, N.; Horozova, E.; *Scientific Papers*, **2005**, 33, Book 5, Chemistry, 55.
11. Haliarnyk, D. M.; Bakalinska, O. M.; Palyanytsya B. B.; Kulyk T. V.; Kartel, M. T.; *Surface*, Kiev: Naukova dumka, **2015**, 7, 253. [in Ukrainian].  
<http://surfacezbir.com.ua/images/Arhiv/N22/27.3.10.pdf>
12. Glevatska, K. V.; Bakalinska, O. M.; Kartel, M. T.; *Transactions of NaUKMA, Chemical Sciences and Technologies*, **2008**, 79, 19. [in Ukrainian].  
[http://ekmair.ukma.edu.ua/bitstream/handle/123456789/6235/Hlevatska\\_Doslidzhennya\\_opys\\_ta\\_porivnyannya\\_katalaznoyi.pdf](http://ekmair.ukma.edu.ua/bitstream/handle/123456789/6235/Hlevatska_Doslidzhennya_opys_ta_porivnyannya_katalaznoyi.pdf)
13. Pokrovskiy, V. O.; *News Nat. Acad. Sci. of Ukraine*, **2012**, 12, 28. [in Ukrainian].  
<http://dspace.nbu.gov.ua/handle/123456789/42699>
14. Schmidt M. W.; Baldrige, K. K.; Boatz, J. A.; Elbert, S. T.; Gordon, M. S.; Jensen, J. H.; Koseki, S.; Matsunaga, N.; Nguyen, K. A.; Su, S. J.; Windus, T. L.; Dupuis, M.; Montgomery, J. A.; *J. Comput. Chem.*, **1993**, 14, 1347.  
DOI: [10.1002/jcc.540141112](https://doi.org/10.1002/jcc.540141112)
15. Becke, A.D.; *J. Chem. Phys.*, **1993**, 98, 5648.  
DOI: [http://dx.doi.org/10.1063/1.464913](https://doi.org/10.1063/1.464913)
16. Lee, C.; Yang, W.; Parr, R. G.; *Phys. Rev. B.*, **1988**, 37, 785.  
DOI: <https://doi.org/10.1103/PhysRevB.37.785>
17. Grimme, S.; Ehrlich, S.; Goerigk, L.; *J. Comput. Chem.*, **2011**, 32, 1456.  
DOI: [10.1002/jcc.21759](https://doi.org/10.1002/jcc.21759)
18. Cossi, M.; Barone, V.; Cammi, R.; Tomasi, J.; *Chem. Phys. Lett.*, **1996**, 255, 327.  
DOI: [https://doi.org/10.1016/0009-2614\(96\)00349-1](https://doi.org/10.1016/0009-2614(96)00349-1)
19. Lyalikov, Yu. S.; *Physico-chemical methods of analysis*; Moskva: Himiya, **1973**. [in Russian].
20. Jensen, F.; *Introduction to Computational Chemistry*. Second Edition; New York: Wiley, **2007**.
21. Kuts, V. S.; Klimenko, V. E.; Strelko, V. V. Cluster Models of Active Carbon, In *Selective Sorption and Catalysis on Active Carbons and Inorganic Ionites*; Strelko, V. V. (ed.); Kiev: Naukova dumka, **2008**, pp. 45–64. [in Russian].